An 868 MHz Bandage Type Antenna using Aluminum conductor and PDMS substrate

Sanjeev Kumar, Roy B. V. B. Simorangkir, Dinesh R. Gawade, Aidan J. Quinn, Brendan O'Flynn and John L. Buckley
Wireless Sensor Networks Group, Tyndall National Institute, Dyke Parade, Cork, Ireland
Email: sanjeev.kumar@tyndall.ie

***Abstract*—This paper presents an 868 MHz ultra-high frequency (UHF) bandage-type antenna for wireless body sensor network applications. The proposed antenna has a modified planar rectangular patch antenna topology and is realized using aluminum metalization and a flexible polydimethylsiloxane (PDMS) substrate. The performance characteristics of the antenna have been investigated through electromagnetic simulations and measurements on a human body phantom arm. The proposed antenna achieves a bandwidth of 11 MHz which is 57 % wider than the required bandwidth for the European LoRaWAN 868 MHz band operation. When compared to bandage-type Sub-GHz antennas reported in the literature, the proposed antenna exhibits desired gain and efficiency performance. Furthermore, the developed antenna demonstrates a low 10-g averaged SAR figure of 0.82 W/kg when 25 mW input power is supplied. The achieved impedance and radiation characteristics make the proposed antenna suitable for a wide range of body-worn wireless health monitoring applications.**

Keywords—aluminum antenna, band-aid, bandage-type antenna, PDMS, Sub-GHz, UHF, wearable antenna.

I. Introduction

In recent times, the rapid progress in human-centric wireless communications has led to an ever-increased interest in on-body wireless sensor devices, such as a bandage-type sensor device for wireless health monitoring applications [1, 2]. The work presented in this paper focuses on the development of a compact bandage-type Sub-GHz antenna for an on-body wireless sensor device operating at the 868 MHz UHF European long-range wide area network (LoRaWAN) frequency band i.e., 863 – 870 MHz [3].

The design of antennas for Sub-GHz bands (e.g., 868 MHz) is challenging primarily because of the practical size constraints of a typical Band-Aid, resulting in an electrically small antenna with limited impedance bandwidth, gain and radiation efficiency. Nonetheless, in the last decade, several bandage-type Sub-GHz antennas that can directly be placed on the human skin have been reported. For example, the on-body 868 MHz UHF radio frequency identification (RFID) antenna reported in [4] achieves a bandwidth of 160 MHz, however, this antenna has a low peak realized gain of -17.1 dBi and an efficiency of approximately 1 %. The meandered on-body monopole antenna reported in [5] achieved a -10 dB impedance bandwidth of more than 300 MHz, but this antenna has a low peak realized gain of -16.98 dBi at 868 MHz. In [6], an 868 MHz RFID patch antenna is reported which has a peak realized gain of -1.44 dBi but at the cost of a narrow bandwidth of less than 4 MHz. The 915 MHz UHF RFID wristband patch antenna reported in [7] achieved a gain of -6.86 dBi, but this antenna does not meet the minimum required bandwidth of 26 MHz for 915 MHz band operation [8, 9].

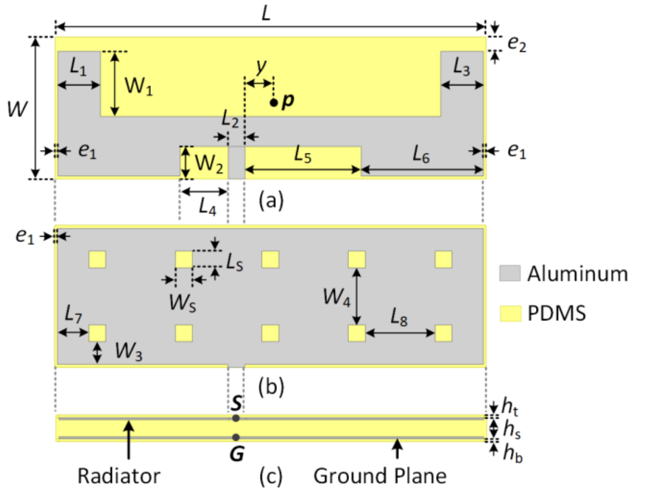

Fig. 1. Configuration of the proposed antenna: (a) Top view, (b) bottom view and (c) side view. Final design parameters: $L = 76$, $L_1 = 7.5$, $L_2 = 3$, $L_3 = 7.5$, $L_4 = 10.5$, $L_5 = 18.5$, $L_6 = 22$, $L_7 = 5.5$, $L_8 = 12.25$, $L_S = 3$, $W = 25$, $W_1 = 12.2$, $W_2 = 5.73$, $W_3 = 4$, $W_4 = 10$, $W_S = 3$, $e_1 = 0.5$, $e_2 = 2.5$, $h_t = 0.2$, $h_s = 1.5$, $h_b = 0.2$, $y = 4.5$, all dimensions are in millimeters.

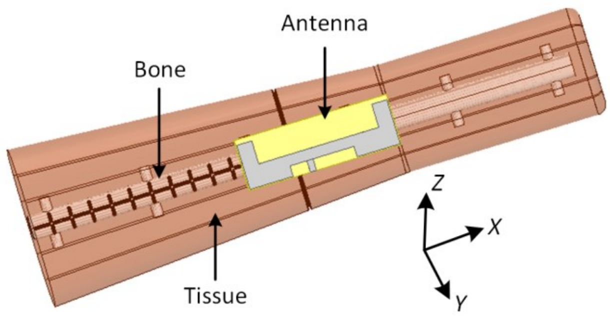

Fig. 2. EM simulation model of the proposed antenna placed on a phantom arm.

It is observed from the literature review that the majority of Sub-GHz bandage-type antennas achieve a wider bandwidth but at the cost of compromised radiation characteristics.

This paper describes the design of a compact bandage antenna with the aim of achieving the required -10 dB impedance bandwidth of 7 MHz for the 868 MHz band (863 – 870 MHz) operation as well as yielding improved radiation performance compared to the literature [10]. Furthermore, bandage-type antennas are desired to be flexible, stretchable, water-resistant and biocompatible to enable seamless and intimate integration with the human skin. Therefore, to achieve the above requirements, the proposed antenna has been realized using a polydimethylsiloxane (PDMS) polymer substrate [11].

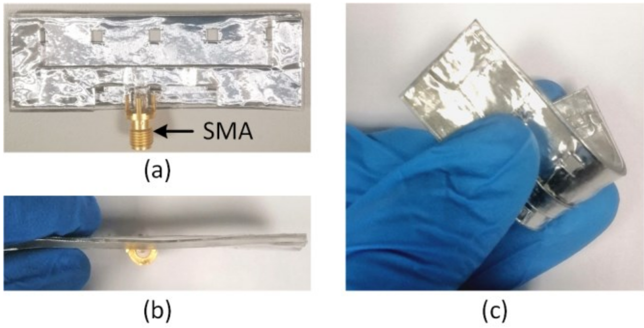

Fig. 3. Fabricated antenna prototype: (a) top view, (b) side view, (c) folded antenna demonstrating its flexibility.

II. Antenna Design and Prototype

The configuration of the proposed antenna is illustrated in Fig. 1. The antenna represents a microstrip patch structure with a full ground plane beneath the radiator to help isolate it from the lossy human body tissue. The overall dimensions of the antenna are 76 mm × 25 mm × 1.9 mm which correspond to free-space electrical dimensions of 0.22 λ_0 × 0.07 λ_0 × 0.005 λ_0, where λ_0 = 346 mm is the free-space wavelength calculated at 868 MHz. As shown in Fig. 1, the antenna is fed with a 50-Ω unbalanced feed at the terminal of the feedline of dimension $L_2 \times W_2$, where the signal is connected at point S and ground at point G. The antenna has a symmetrical structure except for the feedline location. The feedline is situated at a distance y = 4.5 mm away from the centre point p to achieve the desired impedance matching at 868 MHz. The antenna was designed using aluminum with a conductivity of $\sigma = 3.8 \times 10^7$ S/m and a thickness of 0.117 mm on PDMS substrate. At 868 MHz, the PDMS substrate has a relative electrical permittivity $\varepsilon_r = 2.8$ and loss tangent $tan\delta = 0.015$. The entire antenna structure is completely encapsulated into PDMS to make the fabricated antenna robust against any mechanical stress. Furthermore, as shown in Fig. 1(b), ten square-shaped slots were etched in the ground plane to enable PDMS to PDMS bonding [11] that further improves the robustness of the fabricated antenna. As shown in Fig. 2, the electromagnetic (EM) simulation of the antenna was carried out with the antenna placed directly on a phantom arm from Speag [12]. Based on the average electrical properties of the Speag phantom arm at 868 MHz [12], the arm tissue was modelled with $\varepsilon_r = 30$ and $\sigma = 0.7$ S/m, whereas the bone was modelled with $\varepsilon_r = 30$ and $\sigma = 2.5$ S/m.

The photograph of the fabricated antenna is illustrated in Fig. 3 demonstrating the flexibility required for an on-body implementation. As described in [11], the antenna prototyping was performed utilizing an aluminum foil and PDMS, through the bottom-top multilayer fabrication process described in [11]. As shown, for measurement purposes, an SMA connector was soldered to the conductive feedline terminal after partly removing the top and bottom PDMS layers.

III. Antenna Performance

The EM simulation of the antenna was performed using ANSYS HFSS [13]. A parametric analysis of the antenna on phantom was performed with an aim to achieve the minimum required -10 dB impedance bandwidth of larger than 7 MHz while maximizing the antenna radiation performance at 868 MHz. The effects of the key parameters (W_2 and y) on the S_{11} response of the antenna are summarized in Fig. 4.

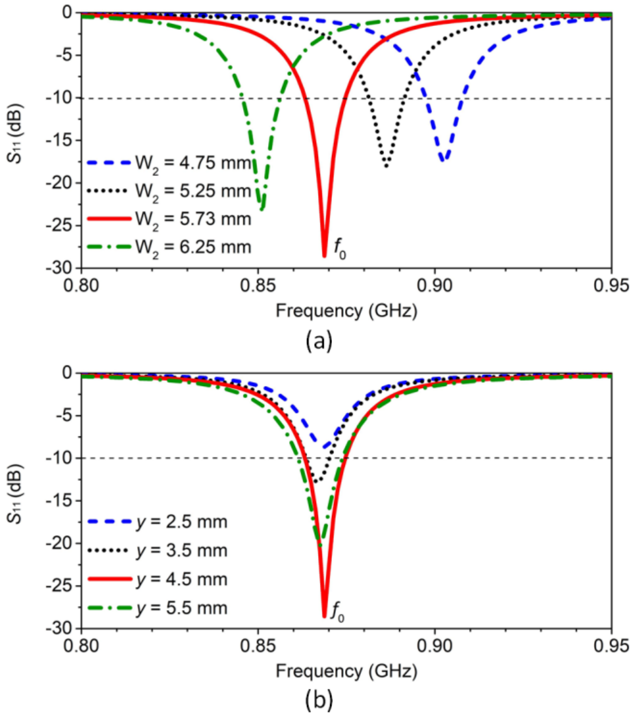

Fig. 4. Simulated S_{11} response of the antenna for varying (a) W_2, (b) y.

In parametric analysis, only one parameter was varied at a time and other parameters were held constant as listed in the caption of Fig. 1. The S_{11} response of the antenna with varying W_2 is summarized in Fig. 4 (a). It can be seen that parameter W_2 primarily affects the resonant frequency f_0 of the antenna and f_0 decreases continuously as W_2 increases from 4.75 to 6.25 mm. The antenna is resonant at f_0 = 868 MHz for W_2 = 5.73 mm. Next, the effect of varying parameter y which represents the feed point location from the center point p of the antenna was investigated. As shown in Fig. 4(b), parameter y predominantly controls the impedance matching and the antenna is well matched at 868 MHz for y = 4.5 mm. The final optimized dimensions of the proposed antenna are listed in the caption of Fig. 1.

The simulated and measured S_{11} response of the developed bandage-type antenna is illustrated in Fig. 5. The S_{11} response of the antenna mounted on the Speag phantom arm was measured using a vector network analyzer (MS2038C) from Anritsu [14]. For the antenna measurement, ferrite beads were used to suppress the effects of coaxial cable currents on the measured antenna characteristics. The S_{11} response in Fig. 5 shows that the antenna achieves a bandwidth of 11 MHz which is 57 % wider than the required -10 dB impedance bandwidth for the target 868 MHz band operation.

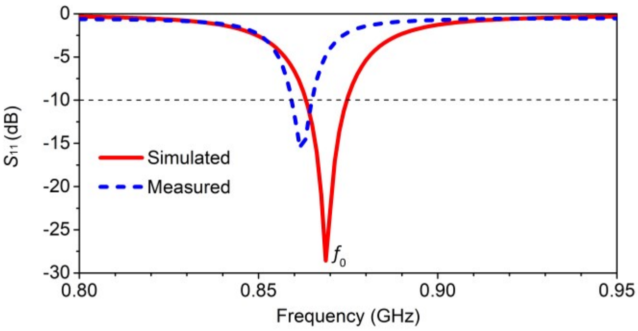

Fig. 5. Simulated and measured S_{11} response of the antenna when placed on the phantom arm.

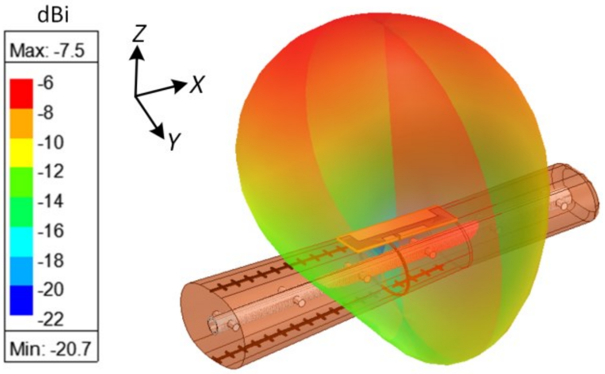

Fig. 6. Simulated 3D radiation pattern of the antenna at 868 MHz.

The discrepancy in the resonant frequency is likely attributed to fabrication inaccuracies.

The simulated 3D radiation pattern of the antenna at 868 MHz is illustrated in Fig. 6. The radiation pattern is similar to a conventional microstrip patch antenna with a peak realized gain of -7.5 dBi at 868 MHz. The antenna exhibits radiation nulls along the negative Z-axis in the *YZ*- and *XZ*-planes which is expected because of the shielding effect of the ground plane. Furthermore, the proposed antenna demonstrates a simulated radiation efficiency of 6.1 % at 868 MHz. In addition, for the maximum permissible effective radiated power level at 868 MHz in Europe i.e. 25 mW [15], this antenna has a peak 10-g averaged specific absorption rate (SAR) of 0.82 W/kg. This SAR figure is less than 21 % of the SAR limit of 4 W/kg defined for limbs [15, 16]. When compared to the literature, the achieved impedance and radiation performance together with the antenna unique mechanical characteristics (i.e., being flexible, lightweight, water-resistant, and biocompatible) demonstrates that the developed antenna is a promising candidate for wearable bandage antennas in wireless health monitoring applications.

IV. Conclusions

In this paper, the design of a compact 868 MHz UHF bandage-type patch antenna is presented. The antenna was realized using aluminum and a flexible PDMS substrate. At 868 MHz the developed antenna has a bandwidth of 11 MHz which is 57 % higher than the minimum -10 dB bandwidth requirements of 7 MHz for the 868 MHz band operation. The simulated results show that the antenna has achieved a peak realized gain of -7.5 dBi and a radiation efficiency of 6.1 % at 868 MHz. Moreover, for an input power of 25 mW, a peak 10-g averaged SAR of 0.82 W/kg was achieved which makes this bandage antenna suitable for a wide range of on-body wireless sensor network applications. Future research will focus on experimental validation of the radiation characteristics of the antenna.

Acknowledgment

The authors would like to acknowledge the support of Enterprise Ireland and the IDA for funding this work under grant IP20170559. We also acknowledge the support from Science Foundation Ireland (SFI): Connect Centre under grant 13/RC/2077 and Insight Centre under grant SFI/12/RC/2289c. The authors would also like to acknowledge the support of Vistamilk under grant 16/RC/3835, Holistics DTIF under Grant EIDT20180291-A and European Regional Development Fund which contributed to aspects of this research work.

References

[1] T. V. Nguyen, H. Okada, Y. Takei, A. Takei, and M. Ichiki, "A Band-Aid Type Sensor for Wearable Physiological Monitoring," in *2021 21st International Conference on Solid-State Sensors, Actuators and Microsystems (Transducers)*, 2021, pp. 1432-1435.

[2] Y. Chi and F. Chen, "On-Body Adhesive-Bandage-Like Antenna for Wireless Medical Telemetry Service," *IEEE Transactions on Antennas and Propagation,* vol. 62, no. 5, pp. 2472-2480, 2014.

[3] R. B. V. B. Simorangkir, D. R. Gawade, S. Kumar, B. O'Flynn, J. L. Buckley, T. Hannon, P. Donovan, and R. Newberry, "Screen Printed Epidermal Antenna for IoT Health Monitoring," in *2021 IEEE Asia-Pacific Microwave Conference (APMC)*, 2021, pp. 395-397.

[4] J. Tribe, D. Oyeka, J. Batchelor, N. Kaur, D. Segura-Velandia, A. West, R. Kay, K. Vega, and W. Whittow, "Tattoo Antenna Temporary Transfers Operating On-Skin (TATTOOS)," in *Design, User Experience, and Usability: Users and Interactions*, Cham, 2015, pp. 685-695.

[5] W. Yang, K. Ma, K. S. Yeo, W. M. Lim, and Z. H. Kong, "A compact dual-band meander-line antenna for biomedical applications," in *2013 IEEE MTT-S International Microwave Workshop Series on RF and Wireless Technologies for Biomedical and Healthcare Applications (IMWS-BIO)*, 2013, pp. 1-3.

[6] M. Feliziani and F. Maradei, "Antenna design of a UHF RFID tag for human tracking avoiding spurious emission," in *2012 IEEE International Symposium on Electromagnetic Compatibility*, 2012, pp. 245-248.

[7] G.-L. Huang, C.-Y.-D. Sim, S.-Y. Liang, W.-S. Liao, and T. Yuan, "Low-Profile Flexible UHF RFID Tag Design for Wristbands Applications," *Wireless Communications and Mobile Computing,* vol. 2018, p. 9482919, 2018/06/07 2018.

[8] S. Kumar, R. Newberry, T. Hannon, J. Barton, M. Rodencal, M. Pigeon, W. G. Scanlon, B. O'Flynn, and J. L. Buckley, "A Bandwidth-Enhanced Sub-GHz Wristwatch Antenna Using an Optimized Feed Structure," *IEEE Antennas and Wireless Propagation Letters,* vol. 20, no. 8, pp. 1389-1393, 2021.

[9] S. Kumar, J. L. Buckley, J. Barton, R. Newberry, G. Dunlop, M. Rodencal, C. Webster, and B. O'Flynn, "A Bandwidth Enhanced 915 MHz Antenna for IoT Wrist-Watch Applications," in *2019 13th European Conference on Antennas and Propagation (EuCAP)*, 2019, pp. 1-5.

[10] S. Kumar, J. L. Buckley, J. Barton, M. Pigeon, R. Newberry, M. Rodencal, A. Hajzeraj, T. Hannon, K. Rogers, D. Casey, D. O'Sullivan, and B. O'Flynn, "A Wristwatch-Based Wireless Sensor Platform for IoT Health Monitoring Applications," *Sensors,* vol. 20, no. 6, p. 1675, 2020.

[11] R. B. V. B. Simorangkir, Y. Yang, and K. P. Esselle, "Robust implementation of flexible wearable antennas with PDMS-embedded conductive fabric," in *12th European Conference on Antennas and Propagation (EuCAP 2018)*, 2018, pp. 1-5.

[12] *Speag phantom arm: SHO-GFPC-V1, (Accessed on 19 January 2022)* Available: https://speag.swiss/products/em-phantoms/overview-2/

[13] *Ansys HFSS, (Accessed on 19 January 2022)*. Available: https://www.ansys.com/products/electronics/ansys-hfss

[14] *Anritsu MS2038C vector network analyzer, (Accessed on 19 January 2022)*. Available: https://www.anritsu.com/en-us/test-measurement/products/ms2038c.

[15] ETSI EN 300 220-2 V3.2.1 (2018-06), Short Range Devices (SRD) Operating in the Frequency Range 25 MHz to 1000 MHz; Part 2: Harmonised Standard for Access to Radio Spectrum for Non Specific Radio Equipment, (Accessed on 19 January 2022). Available: https://www.etsi.org/.

[16] IEEE Standard for Safety Levels with Respect to Human Exposure to Electric, Magnetic, and Electromagnetic Fields, 0 Hz to 300 GHz, *IEEE Std C95.1-2019 (Revision of IEEE Std C95.1-2005/ Incorporates IEEE Std C95.1-2019/Cor 1-2019),* pp. 1-312, 2019.